AJNR

In vivo quantitation of regional cerebral blood flow in glioma and cerebral infarction: validation of the HIPDm-SPECT method.

B Drayer, R Jaszczak, A Friedman, R Albright, H Kung, K Greer, M Lischko, N Petry and E Coleman

In vivo Quantitation of Regional Cerebral Blood Flow in Glioma and Cerebral Infarction: Validation of the HIPDm–SPECT Method

Burton Drayer,[1, 2] Ronald Jaszczak,[1] Allan Friedman,[3] Robert Albright,[1, 2] Hank Kung,[4] Kim Greer,[1] Michael Lischko,[1] Neil Petry,[1] and Edward Coleman[1]

Iodine-123 labeled hydroxyiodopropyldiamine (HIPDm) is a diffusible indicator with an 85%–90% extraction fraction and stable retention in the brain for more than 2 hr. Equilibrium-phase imaging and quantitation using single-photon emission computed tomographic (SPECT) scanning defined a distribution of HIPDm in proportion to regional cerebral blood flow (rCBF). Studies in calves affirmed a close correspondence ($r = 0.97$) in calculated rCBF between HIPDm and microspheres using the tissue deposition–arterial input function microsphere methodology. Using this same mathematical analysis in vivo, reproducible rCBF data within the expected range of normal were obtained on repeated studies in the same nonhuman primate. With a diffuse encephalopathy secondary to subarachnoid blood, a bilaterally symmetric decrease in rCBF was present. A prominent focal decrease in HIPDm accumulation and calculated rCBF was noted with cerebral infarction in the distribution of a ligated middle cerebral artery. Patient studies with glioma revealed diminished HIPDm accumulation due to decreased flow and/or pH in the region of the neoplasm as well as in the associated vasogenic edema and overlying gray matter.

Since the initial application of xenon-133 studies in man [1, 2], new techniques have been sought to characterize regional cerebral blood flow (rCBF) with improved morphologic specificity. The non-radioactive xenon-transmission computed tomographic (CT) method [3] provides excellent anatomic resolution but is somewhat cumbersome due to the stringent requirements of the gas-breathing apparatus, particularly if end-tidal xenon concentration is to accurately reflect the arterial input function. Oxygen-15 techniques using positron emission tomography (PET) require a costly on-site cyclotron and chemistry laboratory [4].

New approaches are therefore being explored to use the far less costly and more widely accessible technique of single-photon emission computed tomography (SPECT) in conjunction with diffusible inert gasses [5] or new classes of iodine-123–labeled radiotracers [6–12]. This study describes the validation of rCBF measurements calculated using one of these iodine-123–labeled radiopharmaceuticals, hydroxyiodopropyldiamine (HIPDm) [13]. We are thus attempting to determine whether rCBF in ml 100 g^{-1} min^{-1} can be determined accurately and reproducibly in living subjects. Although a visual or quantitative analysis of brain distribution is sufficient for defining an abnormality when a focal pathologic process is present, an absolute value for rCBF is necessary if studies are to be compared in different stages of disease or an analysis is to be made of diffuse, bilaterally symmetric pathologic processes (e.g., Alzheimer disease, metabolic encephalopathy).

Materials and Methods

Isotope Detection

The Duke-Siemens SPECT system [14, 15] consists of two opposing large-field-of-view (LFOV) gamma scintillation cameras mounted on a rotatable gantry with each head rotating through 360° in 2–26 min. Our studies use low-energy, all-purpose parallel (LEAP) or medium-energy collimators. Thirty-two contiguous transaxial sections, each 6.4 mm thick, were reconstructed from projection data acquired during a single continuous 360° rotation. The data were also reformatted into longitudinal sections. An internal first-order attenuation correction was applied to the data during the reconstruction to compensate for the effects of gamma ray attenuation. In addition to a visual analysis of the hard film copy, regions of interest (ROI) were selected for computing counts/voxel and ultimately rCBF.

Isotope Preparation

N,N,N'-trimethyl-N'-(2-hydroxyl-3-methyl-5-iodobenzyl)-1,3-propanediamine·HCl (HIPDm) (fig. 1) was synthesized and prepared in kit form [13]. High-purity, no-carrier-added iodine-123 (T½ = 13.3 hr) was made by the ^{127}I (P,5n) ^{123}Xe-^{123}I reaction (Crocker Nuclear Laboratory, University of California at Davis). The radiochemical purity of the labeled HIPDm was greater than 93% and the dose of iodine-123 was 10–14 mCi (370–519 MBq) for animal studies and 5–6 mCi (185–222 MBq) for patients.

HIPDm Characterization

The first pass fraction of ^{123}I-HIPDm extracted by brain tissue was estimated after a bolus infusion of the radiotracer into the internal carotid artery and the monitoring of the initial time activity

---

curve from consecutive 1 sec collections using a gamma camera. The retention of ^{123}I-HIPDm activity in the brain was analyzed using three 26 min SPECT scans obtained in the 8–34, 40–66, and 100–126 min intervals after the intracarotid or intravenous administration of the radiotracer. All baboon (*Papio cynocephalus*) studies were performed in an intubated animal using intravenous sodium pentobarbital anesthesia. The CO_2 concentration in the arterial blood was in the 35–45 torr range.

Cerebral Blood Flow Analysis

If a close correspondence exists between the derived rCBF as determined by carbonized microspheres and HIPDm, the straightforward flow equation based on organ deposition and arterial input sampling [16] can be used for in vivo HIPDm ("metabolic microsphere") studies: $F = (WCi/Ca) \times 100$, where F is the rCBF in ml 100 g^{-1} min^{-1}, W the constant withdrawal rate in ml min^{-1}, Ci the
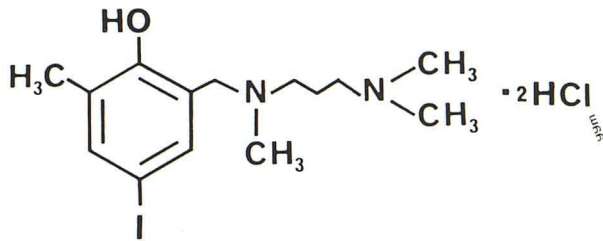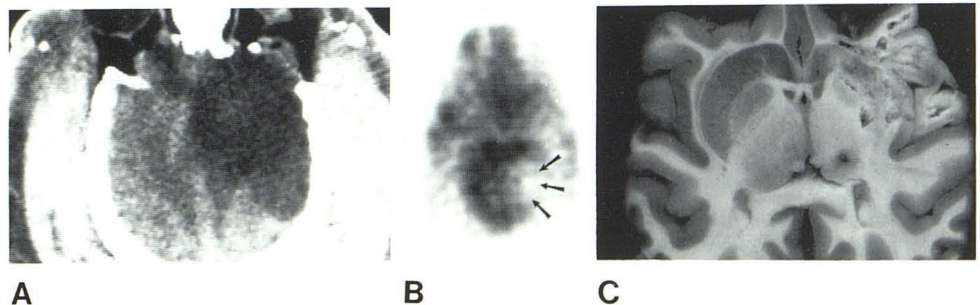

Fig. 1.—N,N,N'-trimethyl-N'-(2-hydroxyl-3-methyl-5-iodobenzyl)-1,3-propanediamine·HCl(HIPDm).

Fig. 2.—[125]I-HIPDm autoradiography. A 12-mm-thick coronal autoradiographic section of cow brain confirms that ^{125}I-HIPDm distribution in brain (gray > white > cerebrospinal fluid) is proportional to rCBF.

activity of ^{123}I-HIPDm in a selected ROI from the SPECT scans in counts sec^{-1} g^{-1}, and Ca the total activity by well-counting in an arterial blood sample constantly withdrawn over the immediate 5 min of radiotracer infusion minus the activity in a 5 min sample begun 10 min after infusion in counts sec^{-1}. A calibration factor to convert well-counter activity to SPECT unit activity is derived by well-counting and SPECT-scanning the blood. "Arterialized" venous blood [17, 18] was drawn from a hand vein after warming to 44°C in a specially designed hand warmer for human studies. Brain activity from chosen ROIs (Ci) was obtained from the 8–34, 40–66, and 100–126 min SPECT scans. In order to compensate for finite resolution and partial volume averaging affecting the mean activity in the selected gray or white matter ROI, we used a simulated brain phantom containing proportional concentrations of iodine-123.

To determine the reproducibility of the SPECT–HIPDm method, the same normal baboon was studied three times at weekly intervals. This same animal was studied again 2 weeks later while diffusely encephalopathic following a retroorbital craniotomy and resulting subarachnoid hemorrhage. After clinical recovery, a fifth study was performed on this animal 2 days after ligation of the left middle cerebral artery producing focal cerebral infarction with neurologic symptomatology.

In order to verify the use of the microsphere paradigm for HIPDm studies, scandium-46 microspheres and iodine-125 HIPDm were injected via a catheter into the left ventricle of the heart in the calf. The animals were killed at 30 min followed by excision of multiple small sections of gray and white matter for well-counting. In addition, arterial blood was drawn at a constant rate over the 0–5 and 10–15 min time intervals. Thick-section autoradiographs were also prepared from 12-mm-thick coronal brain sections to correspond to the SPECT slice thickness.

Human Studies

Four patients with glioma were studied after the infusion of 5–6 mCi (185–222 MBq) of HIPDm. The Ca was determined from arterialized venous blood withdrawn at a constant rate and the Ci from chosen ROIs (25 × 25 mm) on the SPECT scans. All patients had an intravenously enhanced CT study performed to determine tumor localization, blood-brain barrier integrity, and extent of vasogenic edema. A SPECT scan was also obtained to analyze blood-brain barrier integrity using ^{99m}Tc-glucoheptonate and compared with the SPECT-HIPDm rCBF study.

Results

Extraction and Retention

In addition to the brain, the major uptake of HIPDm occurs in the lungs. No significant activity was seen in the eyes. The first pass

Fig. 3.—Cerebral infarction in a baboon 48 hr after surgical ligation of middle cerebral artery (MCA) resulted in profound contralateral hemiparesis, hemianesthesia, and homonymous hemianopsia. **A**, CT. Large area of decreased density in distribution of ligated MCA. **B**, SPECT. Decreased accumulation of HIPDm (*arrows*) in same MCA distribution consistent with decreased rCBF. **C**, Gross pathology. Gross specimen of infarction (*arrows*) in MCA territory.

A   **B**   **C**
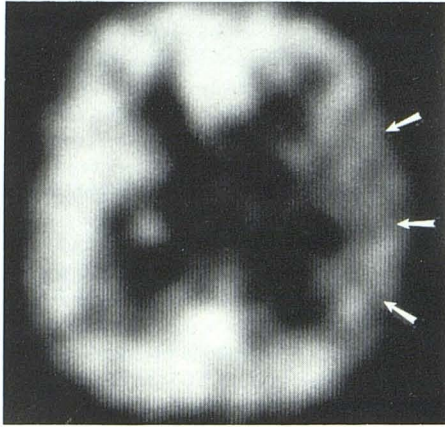
A　　　　　　　　　　**B**

Fig. 4.—Glioblastoma multiforme (GBM) in 53-year-old man. Decreased accumulation of HIPDm (*arrows*) in GBM, associated vasogenic edema, and adjacent parietal gray matter. Milder decrease in HIPDm accumulation (rCBF) in ipsilateral occipital lobe, not involved by tumor or edema. Normal gray-white distribution of HIPDm evident in contralateral hemisphere.
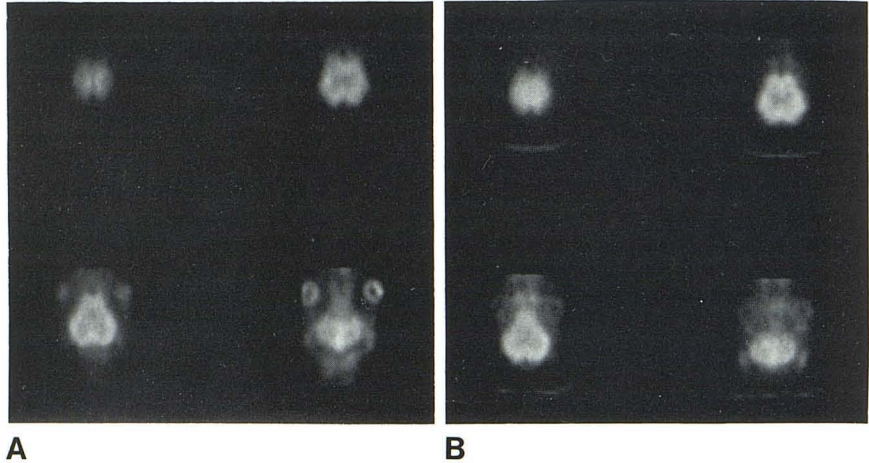
Fig. 5.—Comparative distribution of HIPDm versus microspheres. In vivo comparison in two separate cows after left ventricular infusion of ^{99m}Tc microspheres (A) and ^{123}I-HIPDm (B). Similarity of gray-white distribution is striking in visual and quantitative terms, further affirming mathematical modeling of HIPDm as "metabolic microspheres."

extraction was 85%–90% at a mean CBF of 50–55 ml 100 g^{-1} min^{-1} and pH of 7.35–7.40. The brain activity and the gray-white distribution remained constant in all studies over the 2 hr of scanning. The gray-white distribution in the normal studies was 1.32 ± 0.14 at an approximate spatial resolution of 15 mm FWHM. After phantom compensation, the gray-white ratio was in the 4 to 1 range. This coincided closely with the iodine-125 HIPDm autoradiographic studies (fig. 2), which also demonstrated a distribution of activity in the gray and white matter in proportion to capillary density (i.e., about 4 to 1).

Equilibrium Image Analysis

A visual distinction was consistently present between the gray and white matter. Focal regions of diminished distribution of HIPDm were visually apparent with both cerebral infarction (fig. 3) and glioblastoma multiforme (fig. 4). There was also a less prominent decreased distribution of HIPDm in the occipital lobe (fig. 4) ipsilateral to a glioma involving the more anterior visual pathway. There was a close correspondence between the SPECT scan appearance using technetium-99m microspheres and iodine-123 HIPDm injected into the left ventricle of a calf (fig. 5). In both studies, there was symmetric distribution of activity bilaterally and a distinction of the increased activity in gray matter from the underlying white matter.

Quantitative Analysis of rCBF

A close correlation was obtained when comparing rCBF measured using ^{123}I-HIPDm and ^{46}Sc-microspheres (fig. 6). A Spearman rank correlation was used to determine an r of 0.97 on blood flows from 15–90 ml 100 g^{-1} min^{-1}. Due to this close correspondence, the mathematical modeling developed for use with microspheres was applied to the in vivo HIPDm studies.

The results of serial rCBF estimations in the same baboon on the same day and on different days are summarized in table 1. The phantom-derived compensation factor was 1.73 for regions of cor-
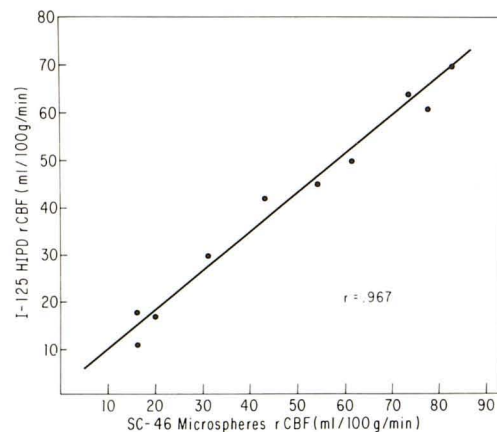

Fig. 6.—Verification of microsphere methodology for HIPDm rCBF estimations. Tight correspondence between ^{46}Sc microspheres and ^{125}I-HIPDm-derived rCBF with flows of 10–90 ml 100 g^{-1} min^{-1} (pH 7.35–7.40). The ^{46}Sc microspheres were infused into left ventricle of the cow immediately after left ventricular infusion of HIPDm.

tical gray matter and 0.59 for white matter locales. Using these compensation factors, the expected 4 to 1 ratio of gray to white matter flow was obtained. A statistically significant difference in gray matter flow in the frontal, temporal, parietal, and occipital lobes was not noted.

When the animal had a diffuse encephalopathy after subarachnoid hemorrhage, a bilaterally symmetric decrease in gray and white matter flow was noted. With cerebral infarction, a prominent, well defined, focal area of diminished HIPDm accumulation was apparent in the distribution of the ligated middle cerebral artery (fig. 3). The extent of severely diminished flow was slightly decreased as compared with the abnormality noted on CT scanning. The contralateral hemisphere showed no abnormality on nonenhanced or intravenously enhanced CT scanning, but exhibited decreased

TABLE 1: **SPECT–HIPDm: Normal and Pathologic rCBF in a Baboon and Pathologic rCBF in a Patient**

	8–33 min Scan					40–66 min Scan					100–125 min Scan				
	Uncorrected		Gray/White Ratio	Corrected		Uncorrected		Gray/White Ratio	Corrected		Uncorrected		Gray/White Ratio	Corrected	
	Gray	White		Gray	White	Gray	White		Gray	White	Gray	White		Gray	White
Baboon Studies:															
Normal, 1	36.8	26.5	(1.34)	64	15	40.4	27.6	(1.46)	70	16	40.7	28.4	(1.43)	70	16
Normal, 2	42.1	31.4	(1.34)	73	18	44.7	34.0	(1.31)	77	19	46.6	39.4	(1.18)	81	23
Normal, 3	46.1	35.1	(1.31)	80	20	48.7	38.8	(1.26)	84	22	50.0	38.7	(1.29)	87	22
With encephalopathy	21.9	13.7	(1.60)	38	8	22.7	13.7	(1.66)	39	8	23.1	15.5	(1.49)	40	9
2 days after infarction	8.8	20.3	(0.43)	15	12	11.5	25.8	(0.45)	20	15	11.5	26.4	(0.44)	20	15
Contralateral hemisphere	29.1	24.7	(1.18)	50	15	29.8	21.7	(1.37)	52	12	26.4	20.7	(1.28)	46	12
Patient with glioblastoma:															
Tumor and edema in frontoparietal area			...			28.3	19.2	(1.47)	49	11			...		
Contralateral hemisphere			...			40.0	26.2	(1.53)	69	15			...		

Note.—Mean (n = 5) rCBF in ml 100 g^{-1} min^{-1} calculated from 25 × 25 mm regions of interest. Coefficient of variation of derived SPECT counts is 5%–11%. Predicted gray/white ratio at 15 mm FWHM = 1.41 ± 0.42 as per Mazziotta et al. [19].

gray matter flow on the SPECT–HIPDm studies, consistent with diaschisis.

In all four patients with high-grade astrocytomas, a decreased accumulation of HIPDm was apparent on the SPECT study (fig. 4). The region of decreased activity was larger than the area of blood-brain barrier abnormality as determined using ^{99m}Tc-glucoheptonate. The SPECT–HIPDm abnormality coincided quite closely, however, with the area of contrast enhancement and associated vasogenic edema as seen on the CT scan. There was decreased uptake of HIPDm not only in the neoplasm, but also in the overlying gray matter and uninvolved ipsilateral occipital lobe. The decrease in calculated flow was less with glioma than with acute infarction (table 1).

Discussion

Studies in animals as well as initial studies in man strongly suggest that the HIPDm–SPECT method will provide useful and reproducible data concerning rCBF. HIPDm crosses the blood-brain barrier with a high first-pass extraction. The radiopharmaceutical is retained in the brain for more than 2 hr at an equilibrium concentration, permitting the acquisition of high-quality images without time restraint. Even though a large amount of the injected dose is trapped by the lungs, about 5%–6% of the injected dose enters the brain. There has been no evidence of toxicity in either mammals or man.

The lipid solubility of HIPDm accounts for its ready permeability across the blood-brain barrier. The mechanism of brain retention is far more complex. Current theories suggest a pH gradient hypothesis in which the nonionized diamine in the blood stream is lipophilic and thus crosses the blood-brain barrier. However, with the lower pH in the brain, the cationic radiotracer is no longer lipophilic and thereby becomes metabolically trapped within the brain substance [7]. Loberg [8] suggests that the pH gradient hypothesis may account for the initial uptake of HIPDm in the brain, however, the final distribution of the agent may be related to other types of metabolism or binding. Additional studies would also be of value to determine whether the small percentage of residual circulating iodine-123 is free, bound to HIPDm, or bound to one of its metabolites.

The high degree of correspondence in postmortem studies using simultaneously injected microspheres and HIPDm confirmed the utility of using the mathematical microsphere methodology for estimating rCBF in vivo using the SPECT–HIPDm paradigm. Due to the excellent retention of HIPDm, blood flow can be calculated at any

time in the first 2 hr after intravenous infusion of the radiopharmaceutical using the equilibrium SPECT image to quantitate brain concentration. The 1.32 ± 0.14 ratio of gray-to-white activity is fully consistent with the computer-simulated data of Mazziotta et al. [19] when the full-width–half-maximum is about 15 mm. The use of a simulated brain phantom provides a useful compensation factor for the underestimation of gray-matter flow and overestimation of white-matter flow derived from the uncorrected SPECT scan data.

As expected, estimated gray-matter flows were decreased symmetrically and bilaterally in the diffusely encephalopathic baboon. There was a prominent decrease in HIPDm accumulation with cerebral infarction in the middle cerebral artery distribution apparent by both visual and quantitative analysis. However, the decrease in flow in the contralateral hemisphere (diaschisis) was not apparent on visual inspection. In this animal with a large cerebral infarction, crossed cerebellar diaschisis was not found. The mechanism of the decrease in HIPDm accumulation needs elucidation as to whether this is a pure flow phenomenon or related to the pH gradient changes.

The mechanism of the diminished accumulation of HIPDm with gliomas is also not straightforward [20]. This decrease in tracer accumulation even in the presence of an abnormality in blood-brain barrier permeability and hypervascularity as determined by angiography suggests that the decreased brain activity may truly represent a decrease in flow rather than or in addition to an abnormality in the pH gradient. Gliomas are known to have decreased metabolic rate with associated anaerobic glycolysis with resulting decrease in oxygen consumption [21]. PET studies have also suggested a mild decreased flow with gliomas [22]. An additional factor is the decreased flow in the surrounding vasogenic edema and overlying cerebral cortex. The decline in rCBF in the region of vasogenic edema may be related to a combination of increase in volume (water) as well as decrease in flow due to compression of the microcirculation.

The HIPDm–SPECT studies showed abnormalities in flow in regions of brain where no structural abnormality was noted by CT scan. The decrease in flow in the structurally uninvolved occipital lobe in the glioma patient with a lesion involving the visual pathway more anteriorly and the contralateral hemisphere with cerebral infarction highlights the additional information concerning the understanding of disease that a blood flow study provides. As with PET scanning, HIPDm–SPECT studies can thus be applied to the analysis of visual, auditory, sensory, or motor activation analysis in man.

Although ^{123}I-HIPDm is an extremely useful radiotracer to measure rCBF, iodine-123 is cyclotron-produced. Its 13.3 hr half-life requires rapid transportion if an on-site cyclotron is not available. If the measurement of brain function using SPECT scanning is to achieve more widespread popularity, the development of a technetium-99m–labeled flow tracer is critical. In affirming the accuracy and reproducibility of the SPECT quantitation of brain activity, the value of such a radiotracer becomes apparent, even at the community hospital level. Until the development of technetium-99m–labeled radiopharmaceuticals for evaluating brain metabolism, iodine-123–labeled compounds can serve as a very useful alternative and provide for a far greater degree of labeling flexibility.

REFERENCES

1. Mallett BL, Veall N. Measurement of regional cerebral clearance rates in man using xenon-133 inhalation and extracranial recording. *Clin Sci* **1965**;29:179–191
2. Obrist WD, Thompson HK, Wang HS, et al. Regional cerebral blood flow estimated by [133]Xenon inhalation. *Stroke* **1975**;6:245–256
3. Drayer BP. Functional applications of CT of the central nervous system. *AJNR* **1981**;2:495–510
4. Frackowiak RS, Lenzi GL, Jones T, et al. Quantitative measurement of regional cerebral blood flow and oxygen metabolism in man using [15]O and positron emission tomography: theory, procedure, and normal values. *J Comput Assist Tomogr* **1980**;4:727–736
5. Kanno I, Lassen NA. Two methods for calculating cerebral blood flow from emission computed tomography of inert gas concentrations. *J Comput Assist Tomogr* **1979**;3:71–76
6. Winchell HS, Baldwin RM, Lin TH. Development of I-123-labeled amines for brain studies: localization of I-123 iodophenylalkyl amines in rat brain. *J Nucl Med* **1980**;21:940–946
7. Kung HF, Blau M. Regional intracellular pH shift: a proposed new mechanism for radiopharmaceutical uptake in brain and other tissues. *J Nucl Med* **1980**;21:147–152
8. Loberg MD. Radiotracers for cerebral functional imaging—a new class. *J Nucl Med* **1980**;21:183–186
9. Kuhl DE, Barrio JR, Huang SC, et al. Quantifying local cerebral blood flow by N-isopropyl-p-(^{123}I)iodoamphetamine (IMP) tomography. *J Nucl Med* **1982**;23:196–203
10. Hill TC, Holman BL, Lovett R, et al. Initial experience with SPECT (single photon computerized tomography) of the brain using N-isopropyl I-123 p-iodoamphetamine: concise communication. *J Nucl Med* **1982**;23:191–195
11. Drayer B, Jaszczak R, Friedman A, et al. Tomographic measurement of regional brain perfusion using hydroxyiodopropyldiamine and single photon emission computed tomography. *Stroke* **1982**;13:12
12. Coleman RE, Drayer BP, Jaszczak RJ. Studying regional brain function: a challenge for SPECT. *J Nucl Med* **1982**;23:266–270
13. Tramposch KM, Kung HF, Blau M. Brain imaging with I-123 labeled diamines: a kit preparation suitable for routine clinical use. *J Nucl Med* **1981**;22:12
14. Jaszczak RJ, Chang LT, Stein NA, et al. Whole-body single-proton emission computed tomography using dual, large-field-of-view scintillation cameras. *Phys Med Biol* **1979**;24:1123–1143
15. Jaszczak RJ, Coleman RE, Whitehead FR. Physical factors affecting quantitative measurements using camera-based single photon emission computed tomography (SPECT). *IEEE Trans Nucl Sci* **1981**;28:69–80
16. Marcus M, Heistad D, Ehrhardt J, et al. Total and regional cerebral blood flow measurement with 7–10, 15, 25, and 50 μm microspheres. *J Appl Physiol* **1976**;40:501–507
17. Goldschmidt S, Light AB. A method of obtaining from veins blood similar to arterial blood in gaseous content. *J Biol Chem* **1925**;64:53–58
18. Phelps ME, Huang SC, Hoffman EJ, et al. Tomographic measurement of local cerebral flucose metabolic rate in humans with (F-18)-2-fluoro-2-deoxy-D-glucose: validation of method. *Ann Neurol* **1979**;6:371–388
19. Mazziotta JC, Phelps ME, Plummer D, et al. Quantitation in positron emission computed tomography: 5. Physical-anatomical effects. *J Comput Assist Tomogr* **1981**;5:734–743
20. LaFrance ND, Wagner HN, Whitehouse P, et al. Decreased accumulation of isopropyl-iodoamphetamine (I-123) in brain tumors. *J Nucl Med* **1981**;22:1081–1083
21. Palpogyi R. Regional cerebral blood flow in patients with intracranial tumors. *J Neurosurg* **1969**;31:149–163
22. Ito M, Lammertsma AA, Wise RJS, et al. Measurement of regional cerebral blood flow and oxygen utilization in patients with cerebral tumors using [15]O and positron emission tomography: analytical techniques and preliminary results. *Neuroradiology* **1982**;23:63–74